Secondary electron emission under electron bombardment from graphene nanoplatelets

Isabel Montero[a,*], Lydya Aguilera[a], María E. Dávila[a], Valentin C. Nistor[b], Luis A. González[b], Luis Galán[b], David Raboso[c], R. Ferritto[d]

[a] Instituto de Ciencia de Materiales de Madrid-CSIC, Spain
[b] Departamento de Física Aplicada, Universidad Autónoma de Madrid, Spain
[c] European Space Agency/ESTEC, Noordwijk, The Netherlands
[d] NanoInnova Technologies, UAM, Cantoblanco, Madrid, Spain

a b s t r a c t

We present novel strategies for obtaining materials with low secondary electron emission under electron beam irradiation for advanced technological applications. Apart from the promising low secondary electron emission yield (SEY) of amorphous carbon coatings deposited on rough surfaces, graphene nanoplatelets are shown to be very effective in reducing the SEY even over flat substrates. Here, we report very low SEY from coatings of graphene platelets exposed to the air, indicating a 60% reduction of the SEY respect to the uncoated flat surfaces. The shape of the SEY curve as a function of primary energy looks like the inverted image of a typical SEY curve.

1. Introduction

Secondary electron emission (SEE) processes under electron bombardment plays an important role in communications satellites, large high-energy particle accelerators, and other technological applications furnishing high-power radio-frequency (RF) fields in vacuum [1,2]. Maximum power handling capabilities of satellite waveguide components are limited by the Multipactor discharge which strongly depends on their SEE properties. The Multipactor effect is a RF discharge or electron cloud in devices working in vacuum, where the exponential electron multiplication by SEE from the walls in resonance with the RF field, distorts this electromagnetic field (the signal) and eventually evolves into the Corona gas discharge damaging and even destroying the RF devices [3,4]. Because of the inevitable presence of critical parts in those RF devices where multipacting resonant conditions cannot be avoided by proper RF field design, the search for materials of low SEY (SEE yield or coefficient, usually under normal incidence) has become an important technological research line. Thus, this research on low-SEY surfaces is directed to mitigating Multipactor effect in space high-power RF devices. SEE is a surface process that it is often not well determined because it depends on the type of material but also on the surface finish: surface contaminants and surface morphology. It is easily and significantly influenced by interactions with environment: exposure to the air, humidity, air contaminants, temperature, etc. In space, it may also be influenced by irradiation with photons, electrons, or ions.

Graphite and sp^2 hybridized amorphous carbon coatings present some of the lowest SEY's found in the literature [5]. In this work, we have also studied the SEE properties of graphene flakes because the graphene systems stand out for their extraordinary electronic and optical properties and their potential industrial applications [6–8]. In addition, in obtaining low-SEY surfaces, a strong surface roughness can reduce dramatically the SEY by what is call secondary electron "suppression" [9]. In spite of the increased emitting surface area and average incidence angle, both favoring SEE, part of this emission impacts on the surface protrusions can be absorbed. The net effect can be partial suppression of the secondary emission by absorption in a degree depending on the surface morphology. In this work, our research on graphene flakes is directed toward the exploration of its novel SEE properties which open up new avenues to nanotechnological applications.

2. Experimental

The SEE experiments were performed in an ultra-high-vacuum (UHV) chamber (10^{-9} kPa), where the incident beam of electrons was generated by an ELG2 Kimball Physics electron gun irradiating the surface of the sample within an energy range of interest, 0–1000 eV. The electron beam incidence is set normal to the sample surface and the total SEY, σ, is then calculated by the relation

$$\sigma = \frac{I_s}{I_p} \quad (1)$$

being $I_s = I_p + I_m$ for charge neutrality on a conductive sample, where I_s is the secondary electrons current (positive), I_p is the primary current (positive), and I_m is the sample current to ground (measured in an electrometer, with the sign of $\sigma - 1$). The sample was biased to −27 V. This system uses a pulsed-beam method, only one single pulse per each measurement for minimizing the dose received by the sample and avoiding surface charging effects. The pulse width of the primary electron beam was 200 ns and the peak current was 4 nA. Sample current was monitored using an oscilloscope and a Femto DHPCA-100 high speed and low-noise current amplifier combination. The incident charge per pulse, Q, was typically about 0.8 fC/cm^2. The surface morphology of the samples was studied by field emission scanning electron microscopy (FESEM), Jeol JSM-6500I. Roughness study (Ra, arithmetic average of the absolute values) was performed in a Dektak 150 Surface Profiler by obtaining surface scans up to 15 mm.

Commercial graphite was used to chemically obtain graphene oxide and reduced graphene oxide. Sodium borohydride ($NaBH_4$) was the reductant of graphene oxide [10]. Graphene nanoplatelets were obtained via liquid exfoliation of graphite [11]. The conductive substrates were Good fellow Al foils of 99.9999% and 99% purity; also carbon tape providing both adhesion and conductivity was used as substrate. The Al foil was chemically etched to produce different surface roughness by passing the sample through an etch bath containing HF, HNO_3, and H_2O in a volume ratio of 1:1:1, for the determined time in the range 0–160 s. Films of amorphous carbon about 20–100 nm thick were deposited on unheated rough Al by dc magnetron sputtering, the target was 99.99% pure graphite.

3. Results and discussion

For obtaining surfaces with very low SEY under electron bombardment, a promising route is to modify the surface roughness [12,13]. This has proved to be very effective for macroscopic roughness in high-energy particle accelerators [14,15]. It should be noted that while roughness size is not relevant in the electron emission "suppression" effect due to roughness, it is important for the high-frequency power dissipation at surfaces in space applications. We have studied the effect of the surface roughness on the SEY parameters. Al substrates were selected to be used as templates because aluminum alloys are standard and dominant materials in space applications. Fig. 1 shows the SEY coefficient as a function of the primary energy for two different aluminum samples exposed to the air, the SEY of graphite and adhesive carbon are also included for comparison purposes. We can observe that for aluminum foil, SEY maximum is higher than two (exposed to the air); on the other hand, graphite is a low-SEY material, 1 < SEY < 1.5, less reactive than Al, and should be less affected by air exposure. The effect of different acid etching times on the surface roughness of aluminium samples is shown in Fig. 2. The profile roughness parameter Ra increases as a function of the chemical etching time up to about 35 μm for 150 s and the FE-SEM images (inserted in Fig. 2) reveal the progressive formation of surface pores. Fig. 3 shows the SEY of the Al foil as a

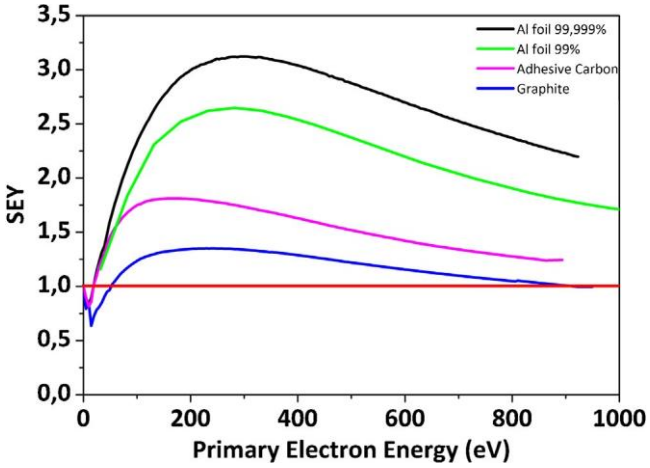

Fig. 1. Secondary electron emission yield (SEY) of two commercial Al foils (99.9999% and 99% purity), adhesive carbon and graphite.

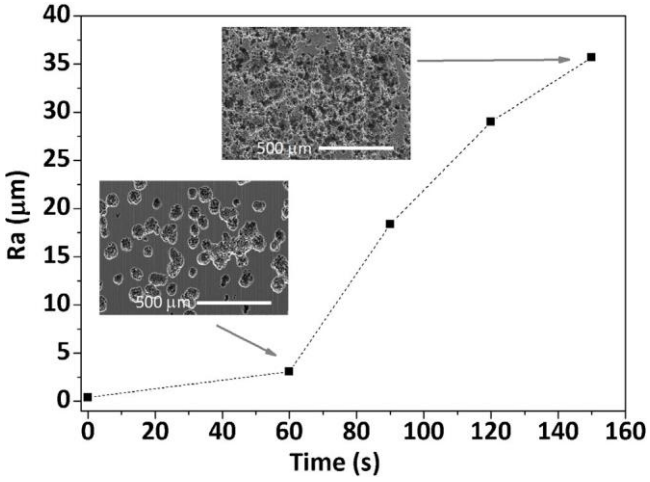

Fig. 2. Average roughness Ra of the Al foil as a function of the chemical etching time. The inserts are FE-SEM images of the Al foil after chemical etching treatment.

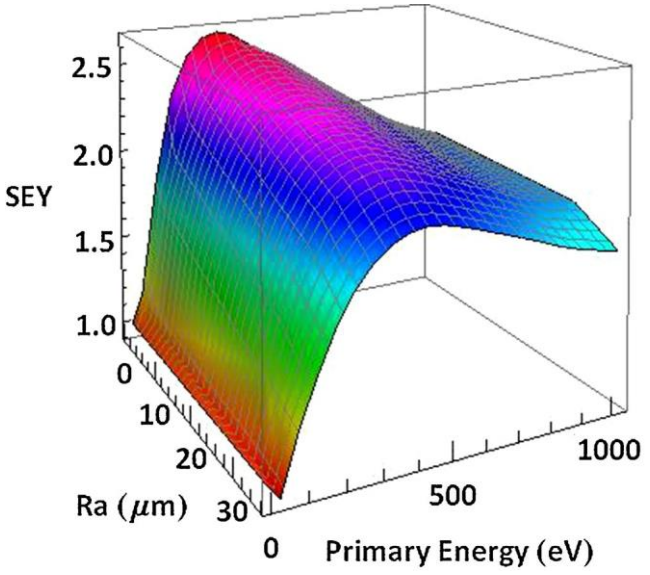

Fig. 3. SEY of Al foil as a function of primary electron energy and roughness Ra.

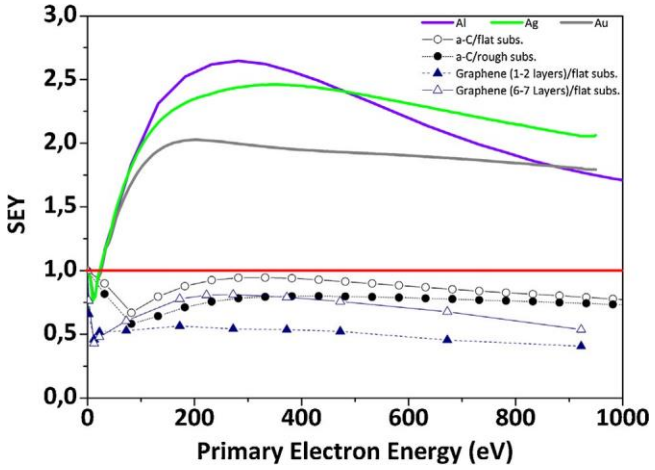

Fig. 4. SEY curves of a-C/rough substrate, and graphene (1–2 layers) and graphene (6–7 layers) deposited on flat substrates. SEY curves of Al, Ag, and Au foils exposed to the air have been included for comparison purposes.

function of the primary energy and surface roughness Ra. In this Figure, it can be seen that SEY decreases with surface roughness; this is due to a "shadow" effect of the walls of the surface pores. Experimental results for Cu and Ag have been reported [16,17] showing a dependence of work function on surface roughness parameter, due to rougher surfaces having lower constraints for electrons to escape from surface sharp peaks, resulting in lower work function which should increase SEY. This is clearly a size effect in part. However, this effect is either not present or canceled by the "emission suppression effect" of the rough Al surfaces, because in our case, roughness parameters were at least one order of magnitude larger than those of references [16,17].

The rough Al substrates were used as templates for preparing carbon surfaces with strong reduction of the SEY. The SEY results of a-C/rough Al (Ra = 15 μm) together those of representative metals (Al, Ag and Au foils) are shown in Fig. 3. FE-SEM and AFM images of a-C/rough Al are presented in Fig. 4a and b. We can observe that a-C/rough Al shows a SEY less than one. This seems a promising route for synthesizing large-area micro structured surfaces with high aspect ratio to obtain low-SEY surfaces, which are difficult to form by conventional deposition process.

However, despite the fact that for many technological applications, the SEY of air-exposed surfaces is more relevant than the SEY of atomically clean surfaces, SEY data for air-exposed surfaces are rare and the reasons for the SEY variation during air exposure of atomically clean metals are still discussed controversially. It is difficult to define an air-exposed surface precisely because of the many parameters influencing the surface properties (e.g. initial sample state, air exposure time, humidity, concentration of contaminants in the ambient air, etc.). Moreover, the SEY of such surfaces is much more sensitive to electron irradiation than the SEY of atomically clean surfaces. Therefore, measurements on air-exposed metal surfaces provide in some cases the SEY of an electron-beam-damaged surface, which has a much lower SEY than the as-received surface. Thin absorbed layers of H_2O may enhance the SEY up to 50% whereas the growth of a graphitized polymerized hydrocarbon layer may reduce the SEY.

The morphology of the graphene nano and microplatelets was studied using FE-SEM microscopies. Apart from the numerous astounding properties of graphene, another remarkable property of graphene flakes is their propensity to stick together. FE-SEM images of Fig. 5c and show the typical random arrangement of graphene flakes, and the particle size of a graphene flakes is in the range of 0.1–1 μm (obtained by TEM).

We have studied the SEY properties of graphene flakes exposed to the air. The difficulty in flattening out those flakes once crumpled could make complicated working with graphene and limit other potential applications. However, this rough surface of graphene flakes can be well suited for reducing the secondary electron emission. Fig. 4 shows the SEY, as a function of the primary energy of films of 1–2 and 6–7 layers of graphene flakes, both deposited on flat substrates. In spite of this flat substrate, we can observe that graphene (1-–2 flake layers thick) shows very low SEY compared to that of a-C/rough substrate. The total number of secondary electrons depends on the work function [18] and it is known that

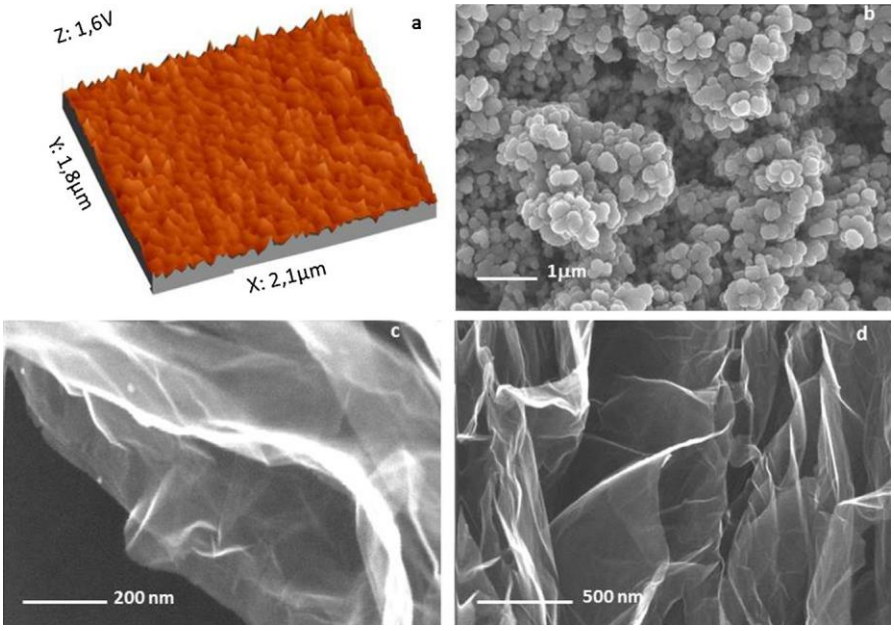

Fig. 5. AFM image of a-C deposited on flat Al (a) and FE-SEM images of a-C deposited on rough Al (b) and graphene crystallites (1–2 layers) deposited on flat surfaces (c and d).

work function of graphene flakes decrease for decreasing number of flakes, from 4.6 eV for 4 or greater, to 4.3 eV for monolayer graphene [19]. It is also well known its exceptionally large values of electron mobility and mean free path [20]. These properties would produce a high SEY material, but graphene is not a bulk material and the SEE process involves always the contribution of the substrate material. Depending on the conductivity of the substrate and the interface, its SEY can be decreased [21,22]. These results indicate the potential of graphene flakes for inhibiting Multipactor.

4. Summary and conclusions

The search of low-SEY materials based on their chemical and physical properties has limitations due to the strong requirements of stability in air. Another newer strategy is based on surface morphology. Strong surface roughness of high aspect ratio shows a secondary emission "suppression" effect due to its partial absorption by the surface protrusions. Both approaches can conveniently be combined in amorphous graphitic carbon films on porous aluminum substrates obtained by chemical etching.

We have found a remarkable low SEY of the nanostructured surface of films of graphene flakes. These results are due to its electronic structure and surface morphology and indicate its potential for application in anti-multipactor coatings for high-power RF devices in space.

Acknowledgements

This work was supported by the European Space Agency (ESA) and MICIIN of Spain Projects No. AYA2009-14736-C02-01 and AYA2009-14736-C02-02.

References

[1] P. Costa Pinto, S. Calatroni, P. Chiggiato, H. Neupert, W. Vollenberg, E. Shaposhnikova, M. Taborelli, C. Yin Vallgren, Proc. 2011 Particle Accelerator Conference, New York, NY, USA, 2011.
[2] J. de Lara, F. Perez, M. Alfonseca, L. Galan, I. Montero, E. Roman, E. Raboso, IEEE Trans. Plasma Sci. 34 (2) (2006) 476–484.
[3] (a) R.A. Kishek, Y.Y. Lau, L.K. Ang, A. Valfells, R.M. Gilgenbach, Phys. Plasmas 5 (1998) 2120;
(b) D. Cai, M. Song, C. Xu, Adv. Mater. 20 (2008) 1706.
[4] R. Udiljak, D. Anderson, M. Lisak, V.E. Semenov, J. Puech, Phys. Plasmas 14 (2007) 033508.
[5] C. Yin Vallgren, S. Calatroni, P. Costa Pinto, A. Kuzucan, H. Neupert, M. Taborelli, Proceedings of IPAC-2011, San Sebastián, Spain, 2011.
[6] A.K. Geim, K.S. Novoselov, Nat. Mater. 6 (2007) 183–191.
[7] K.S. Novoselov, A.K. Geim, S.V. Morozov, D. Jiang, Y. Zhang, S.V. Dubonos, I.V. Grigoriev, A.A. Firsov, Science 306 (2004) 666.
[8] D. Cai, M. Song, C. Xu, Adv. Mater. 20 (2008) 1706.
[9] L. Galán, V. Nistor, I. Montero, L. Aguilera, D. Wolk, U. Wochner, D. Raboso, Proc. MULCOPIM' 2008. ESTEC-ESA, Noordwijk, The Netherlands, 2008.
[10] H.J. Shin, K.K. Sim, A. Benayad, S.-M. Yoon, H.K. Park, I.-S. Jung, M.H. Jin, H.K. Jeong, J.M. Kim, J.Y. Choi, Y.H. Lee, Adv. Funct. Mater. 19 (2009) 1987–1992.
[11] U. Khana, A. O'Neilla, H. Porwal, P. May, K. Nawaz, N. Jonathan, Colema, Carbon 50 (2012) 470–475.
[12] L. Aguilera, I. Montero, M.E. Dávila, A. Ruiz, L. Galán, V. Nistor, D. Raboso, J. Palomares, F. Soria, J. Phys. D: Appl. Phys. 46 (16) (2013) 165104.
[13] L. Aguilera, I. Montero, M.E. Davila, J.L. Sacedon, V. Nistor, L. Galan, D. Raboso, S. Anza, C. Vicente, J. Gil, Proc. MULCOPIM'11, Valencia, Spain, 2011 (European Space Agency).
[14] M.T.F. Pivi, F.K. King, R.E. Kirby, T.O. Raubenheimer, G. Stupakov, F. Le Pimpec, SLAC-PUB-13020, 2007, pp. 1–18.
[15] Y. Suetsugu, H. Fukuma, K. Shibata, M. Pivi, L. Wang, Proc. IPAC'10, 2010, pp. 2021–2023.
[16] W. Li, D.Y. Li, J. Chem. Phys. 122 (6) (2005) 064708.
[17] Y. Wan, Y. Li, Q. Wang, K. Zhang, Y. Wu, Int. J. Electrochem. Sci. 7 (2012) 5204–5216.
[18] M.S. Chung, T.E. Everhart, J. Appl. Phys. 45 (2) (1974) 707.
[19] H. Hibino, H. Kageshima, M. Kotsugi, F. Maeda, F.Z. Guo, Y. Watanabe, Phys. Rev. B 79 (2010) 125437.
[20] A. Geim, S. Novoselov, Nat. Mater. 6 (2007) 183–191.
[21] C. Jacques, Appl. Phys. Lett. 98 (2011) 013109.
[22] P. Riccardi, A. Cupolillo, M. Pisarra, A. Sindona, L.S. Caputi, Appl. Phys. Lett. 101 (2012) 183102.